

Article

Fabrication and Characterization of Polysaccharide Metallohydrogel Obtained from Succinoglycan and Trivalent Chromium

Dajung Kim ¹, Seonmok Kim ¹ and Seunho Jung ^{1,2,*}

¹ Department of Bioscience and Biotechnology, Microbial Carbohydrate Resource Bank (MCRB), Konkuk University, Seoul 05029, Korea; dajung903@naver.com (D.K.); gkdurk9999@naver.com (S.K.)

² Center for Biotechnology Research in UBITA (CBRU), Institute for Ubiquitous Information Technology and Applications (UBITA), Department of Systems Biotechnology, Konkuk University, Seoul 05029, Korea

* Correspondence: shjung@konkuk.ac.kr; Tel.: +82-2-450-3520

Abstract: In the present study, a polysaccharide metallohydrogel was successfully fabricated using succinoglycan and trivalent chromium and was verified via Fourier transform infrared spectroscopy, differential scanning calorimetry analysis, thermogravimetric analysis (TGA), field emission scanning electron microscopy, and rheological measurements. Thermal behavior analysis via TGA indicated that the final mass loss of pure succinoglycan was 87.8% although it was reduced to 65.8% by forming a hydrogel with trivalent chromium cations. Moreover, succinoglycan-based metallohydrogels exhibited improved mechanical properties based on the added concentration of Cr³⁺ and displayed a 10 times higher compressive stress and enhanced storage modulus (G') of 230% at the same strain. In addition, the pore size of the obtained SCx could be adjusted by changing the concentration of Cr³⁺. Gelation can also be adjusted based on the initial pH of the metallohydrogel formulation. This was attributed to crosslinking between chromium trivalent ions and hydroxyl/carboxyl groups of succinoglycan, each of which exhibits a specific pH-dependent behavior in aqueous solutions. It could be used as a soft sensor to detect Cr³⁺ in certain biological systems, or as a soft matrix for bioseparation that allows control of pore size and mechanical strength by tuning the Cr³⁺ concentration.

Keywords: hydrogels; succinoglycan; trivalent chromium; metallohydrogel; rheological properties



Citation: Kim, D.; Kim, S.; Jung, S. Fabrication and Characterization of Polysaccharide Metallohydrogel Obtained from Succinoglycan and Trivalent Chromium. *Polymers* **2021**, *13*, 202. <https://doi.org/10.3390/polym13020202>

Received: 23 December 2020

Accepted: 5 January 2021

Published: 8 January 2021

Publisher's Note: MDPI stays neutral with regard to jurisdictional claims in published maps and institutional affiliations.



Copyright: © 2021 by the authors. Licensee MDPI, Basel, Switzerland. This article is an open access article distributed under the terms and conditions of the Creative Commons Attribution (CC BY) license (<https://creativecommons.org/licenses/by/4.0/>).

1. Introduction

Microbial extracellular polysaccharides (EPS) are biodegradable and biocompatible polymers with the potential to replace petroleum-derived substances, such as acrylic fiber and polyurethane. Their ability to transform into porous-forming gels is attracting significant attention [1–3]. Polysaccharide-based gels are used in various applications including catalyst support, drug delivery agents, and water production control [4–7]. Additionally, EPS has scientific and commercial requirements owing to its wide range of industrial applications and biological properties. They are extensively used in the food industry as gelling and thickening agents, emulsifiers, and texture modifiers to replace commercial hydrocolloids [8,9]. Various applications of microbial EPS, such as chitosan, alginate, galactan, pullulan, curdlan, xanthan, and gellan are widely reported [10–15]. Succinoglycan is an acidic extracellular polysaccharide of octasaccharide that consists of a 1:7 ratio of galactose and glucose and is produced by soil bacteria such as *Sinorhizobium* and *Agrobacterium*. It also contains non-carbohydrate substituents including succinate, pyruvate, and acetate groups [16–18]. It is resistant to high temperatures and high salt or ionic concentrations and has high viscosity [19]. This property of succinoglycan holds immense potential in commercial applications such as cosmetics and household products, fertilizer formulations, pharmaceuticals, emulsifiers, gelling agents, stabilizers, and thickeners [20].

An approach to extend the functionality of polysaccharide hydrogels involves using dynamic non-covalent interactions via crosslinking through metal ions [21], and several

studies examined gelation via the co-ordination of various acidic polysaccharides and metal ions [22–27]. Diverse multivalent metal ions, such as Fe^{3+} , Al^{3+} , Ca^{2+} , Cu^{2+} , Mn^{2+} , Co^{2+} , and Cr^{3+} (which can be co-ordinated with the functional groups of acidic polysaccharides), have been reported [22]. For example, alginate is the most widely examined acidic polysaccharide and creates a specific gelling structure, termed as the “egg-box” model, by the interaction of Ca^{2+} and carboxylic groups of guluronate blocks [28]. In addition to Ca^{2+} , transition metal ions, such as Fe^{3+} , were also observed to form metallohydrogels with alginates [29,30], where metal co-ordinations provide new mechanical properties by controlling the metal co-ordination conditions [31]. Carboxymethyl chitosan-metal ions (e.g., Ag^+ , Cu^{2+} , and Zn^{2+}) hydrogels exhibit excellent antibacterial activity against *S. aureus* and *E. coli* and display enhanced mechanical behavior [32]. Other microbial acidic polysaccharides, gellan [33], salectan [34], and xanthan [35,36] also show that divalent or trivalent cations can induce gelation via chemical crosslinking between carboxylic ($-\text{COO}^-$) groups and metal ions. In particular, xanthan and salectan enhance metallo-gelation by adding trivalent chromium cations [34–36]. Moreover, Cr^{3+} is widely considered to exhibit significantly lower toxicity than Cr^{6+} [37–39]. Therefore, several application studies involving living cells using Cr^{3+} are also reported [40–42].

A salectan-based hydrogel co-ordinated with Cr^{3+} as a crosslinking agent affects the expansion capacity, pore size, and mechanical strength of the hydrogel by changing the Cr^{3+} concentration [34]. In the study of xanthan/ Cr^{3+} systems, the gelation time changed based on the change in pH [43], where the properties of these crosslinks, formed primarily through the formation of chemical bonds between the Cr^{3+} and acidic carboxylic ($-\text{COO}$) groups of xanthan, were relatively strong [44]. Therefore, this pH-controllable gelation in xanthan-based metallohydrogels suggests a potential application to selectively block water during oil recovery operations [45]. Given that succinoglycan has many carboxyl groups as non-carbohydrate substituents that can be potential functional groups via metal co-ordination, it also exhibits the potential to serve as succinoglycan-based metallohydrogels with metal ions.

In this paper, we report the characteristic properties of succinoglycan metallohydrogels (SCx) induced by trivalent chromium (Cr^{3+}). Various investigations, such as rheometry, Fourier transform infrared (FTIR) spectroscopy, X-ray diffraction measurements (XRD), thermogravimetric analysis (TGA), differential scanning calorimetry (DSC), and field emission scanning electron microscopy (FESEM), were performed to characterize SCx.

2. Materials and Methods

2.1. Materials

Sinorhizobium meliloti Rm1021 was supplied by the Microbial Carbohydrate Resource Bank at Konkuk University, Korea. Chromium(III) chloride hexahydrate (95%) was purchased from Daejung Chemicals & Metals Co., Ltd. (Siheung, Korea). All other chemicals were of analytical grade and used without further purification. To vary the pH of the samples, sodium hydroxide (Daejung Chemicals & Metals Co., Ltd., Siheung, Korea, 97%) and hydrochloric acid, as a titration standard for preparation of 1 M or 0.1 M solution (Daejung Chemicals & Metals Co., Ltd., Siheung, Korea, 35–37%), were used.

2.2. Growth Conditions and Production of Succinoglycan

Succinoglycan was isolated and purified from *S. meliloti* Rm1021, as previously described. Bacteria were cultured in glutamic acid-mannitol-salts medium, which was adjusted to a pH of 7.00 at 30 °C for 7 days with shaking (180 rpm). After 7 days, the cells were centrifuged at $8000 \times g$ for 15 min at 4 °C, and the supernatant was collected. Three volumes of ethanol were added to the supernatant to obtain succinoglycan. Furthermore, succinoglycan was first precipitated, and the precipitate was subsequently dissolved in distilled water and then dialyzed (MWCO 12–14 kDa, distilled water for 3 days). After collection, the purified succinoglycan was freeze-dried for later use. The molecular weights of succinoglycan were estimated via gel permeation chromatography (GPC) analysis performed at 30 °C.

GPC was performed using a Waters Breeze System equipped with a Waters 1525 Binary pump and a Waters 2414 refractive index detector using 0.02 N sodium nitrate as a solvent at a flow rate of 0.8 mL min⁻¹. The molecular weight (Mw) of succinoglycan—as estimated via GPC—is 1.8 × 10⁵ Da, as listed in Table S1.

2.3. Preparation for Gelation Confirmation Experiment

To examine the effect of various metal ions, stock aqueous solutions of succinoglycan (aq, 2%) and 0.25 M of KCl, NaCl, CaCl₂, MgCl₂, CuCl₂, ZnCl₂, AlCl₃, FeCl₃, and CrCl₃ were prepared. The metal ionic solution was added to the prepared succinoglycan solution and stirred for 3 min. The resulting mixture was poured into a mold and left for 24 h.

2.4. Preparation of Hydrogels

Succinoglycan solution (aq, 2%) was mixed with an equal volume of Cr³⁺ aqueous solution. Additionally, Cr³⁺ aqueous solution (final 6.6–52.8 mM) was prepared by dispersing a defined amount of CrCl₃ 6H₂O in deionized water under moderate stirring. It was then left for 1 day to realize hydrolysis. The final stock solution exhibited a purple–green color. The mixture was stirred at room temperature for 3 min and then left for at least 18 h to spontaneously form succinoglycan/Cr³⁺ co-ordination hydrogels. The resulting metallohydrogel was formed by mixing an aqueous succinoglycan solution with a Cr³⁺ aqueous solution. It was labeled as SCx, where x corresponded to 6.6, 13.2, 26.4, and 52.8 denoting 6.6, 13.2, 26.4, and 52.8 mM of Cr³⁺ molar concentrations, respectively. A small amount of acid or alkali (0.1 M HCl or 0.1 M NaOH) was added to the gel initially obtained at pH 5 to determine the effect of pH on gelation. Moreover, the effect of pH on uncrosslinked succinoglycan solutions was investigated by adding HCl and NaOH to a mixture of succinoglycan and Cr³⁺ initially obtained at pH 1 and pH 9.

2.5. Fourier Transform Infrared (FTIR) Spectroscopy

The FTIR spectra of the lyophilized succinoglycan and SCx were recorded via an FTIR spectrometer (Spectrum Two FT-IR, Perkin Elmer, Waltham, MA, USA) with a PIKE MIRacle ATR accessory at a resolution of 1 cm⁻¹ using eight scans in the wavenumber range of 4000–600 cm⁻¹.

2.6. X-ray Diffraction Measurements (XRD)

The XRD pattern was measured via a Rigaku SmartLab 9 kW X-ray diffractometer, and a HyPix-3000 was used as the detector for analysis. Samples were used after lyophilization. Tests were performed at 30 kV and 20 mA, and scans were performed in the 2θ range of 10–80 °C.

2.7. Thermogravimetric Analysis (TGA)

Thermogravimetric analysis (TGA) was performed using a Perkin Elmer Pyris1 thermogravimetric analyzer. The thermal analyzer was operated under nitrogen atmospheric pressure and regulated by compatible PC commands. The dried sample (10 mg) was placed in a crucible and heated in an enclosed system with a linear temperature increase at a rate of 10 °C/min over a temperature range of 25 to 600 °C.

2.8. Differential Scanning Calorimetry (DSC)

DSC was performed via a Discovery DSC apparatus (TA Instruments, New Castle, DE, USA). The DSC samples (10 mg) were weighed on an aluminum pan and the pan was sealed. The sample was scanned under a purified nitrogen atmosphere at a heating rate of 10 °C/min from 25 to 180 °C.

2.9. Field Emission Scanning Electron Microscopy (FESEM)

The cross-sectional morphologies of pure succinoglycan and SCx were observed via FESEM (JSM-7800F Prime, JEOL Ltd., Akishima, Japan). The samples were rapidly frozen

and lyophilized for 24 h. For observation, the surface of the cross-sectioned hydrogel was coated with a thin layer of platinum at 10 mA for 60 s in vacuum to render them electrically conductive.

2.10. Rheological Experiments

The rheological properties of the hydrogels were analyzed via oscillation angular frequency sweep and temperature ramp tests of succinoglycan solution that were performed using a DHR-2 rheometer (TA Instruments, New Castle, DE, USA) equipped with 20 mm parallel plates. The angular frequency was swept from 0.1 to 100 rad/s at a strain of 0.5% at a constant angular frequency of 10 rad/s and a constant strain of 1.0%. A stress–strain amplitude sweep test was conducted on samples from 0.1% to a maximum strain of 100% at 1.0 Hz to determine the limit of the linear viscoelastic region. Each measurement was performed in triplicate.

2.11. Compressive Test

With respect to the compressive test, hydrogel discs with a height of 10 mm and a diameter of 20 mm were prepared. Furthermore, compressive tests were performed using an Instron E3000LT (Instron Inc., Norwood, MA, USA). The sample was placed on a plate and compressed at a rate of 5 mm/min. Compressive stress was recorded when the sample was compressed with a strain of 40%. The measurement was performed in triplicate.

2.12. Equilibrium Swelling Ratio

The dried metallohydrogel samples were precisely weighed and immersed in deionized water at 25 °C. At each predetermined time interval, the SCx was removed from the swelling medium and weighed after removing excess surface water. The measurement was continued until constant weights of the swollen metallohydrogels were obtained. The water swelling ratios were calculated as follows [46]:

$$\text{Swelling ratio} = \frac{W_s - W_d}{W_d} \quad (1)$$

where W_s denotes the weight of the swollen hydrogel, and W_d denotes the weight of the dried hydrogel. Each measurement was performed in triplicate.

2.13. UV–Vis Spectrophotometer

A UV–Vis spectrophotometer (UV 2450, Shimadzu Corporation, Kyoto, Japan) was used to confirm that chromium ions were released after immersing the SCx in distilled water (D.W), and spectra were observed from 200 to 700 nm at 2-h intervals over 48 h.

3. Results

3.1. Fabrication of Metallohydrogels

Various aqueous metal ionic solutions, including K^+ , Na^+ , Ca^{2+} , Mg^{2+} , Cu^{2+} , Zn^{2+} , Al^{3+} , Fe^{3+} , and Cr^{3+} , were prepared to determine metal ions capable of forming hydrogels mixed with an aqueous succinoglycan (Figure 1) solution. Figure 2a shows the results of the inverted vial tests for each mixed solution corresponding to the different metal ions. Most metal ions, with the exception of Fe^{3+} and Cr^{3+} , did not induce physical gels. However, stronger physical gel formation was observed only when the Cr^{3+} solution was added to the succinoglycan aqueous solution when compared to the Fe^{3+} solution. Furthermore, this was confirmed by measuring the difference between the storage modulus (G') and loss modulus (G'') via rheological experiments (Figure 2b). The result showed that succinoglycan induce effective metallohydrogel formation by adding Cr^{3+} cations. As listed in Table 1, a succinoglycan-based metallohydrogel is prepared and labeled as SCx, where x corresponds to the aqueous Cr^{3+} molar concentration.

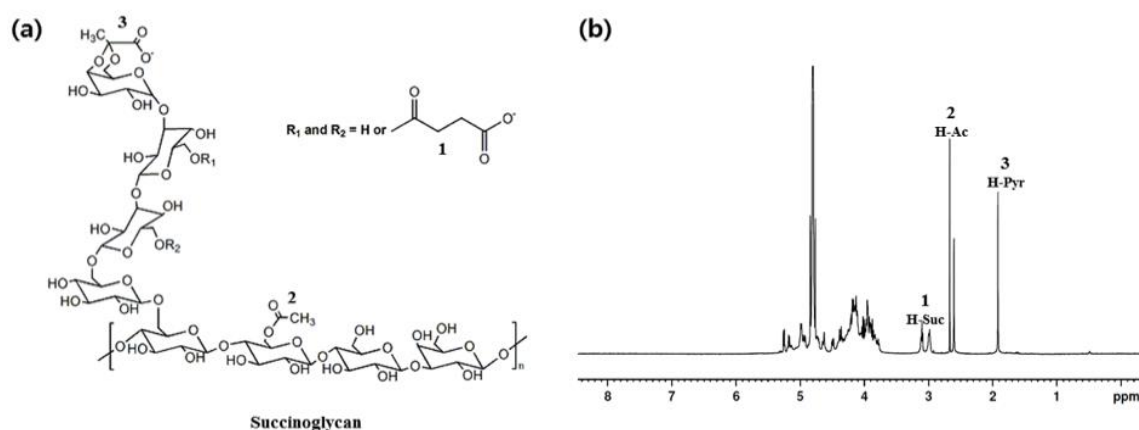


Figure 1. Structure of (a) succinoglycan and (b) ¹H-NMR spectrum of succinoglycan.

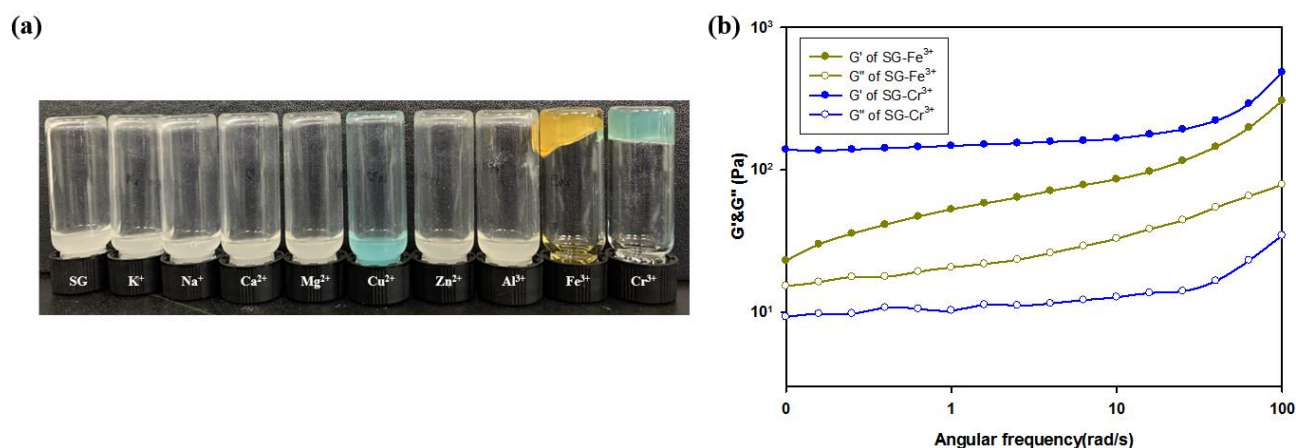


Figure 2. Gelling performance of succinoglycan (SG) with respect to the addition of various metal ions: (a) Inverted vial test after mixing various metal ion solutions (0.25 M) with aqueous succinoglycan solution (wt. 2%), and (b) Frequency sweep of aqueous SG solution containing metal ions (SG-Fe³⁺ and SG-Cr³⁺).

Table 1. Composition of SCx.

Sample Name	Succinoglycan (wt %)	Cr ³⁺ (mM)
SC _{6.6}	1	6.6
SC _{13.2}	1	13.2
SC _{26.4}	1	26.4
SC _{52.8}	1	52.8

3.2. Characterization of Metallohydrogels

The preparation of metallohydrogel was confirmed via FTIR analysis [47]. The metallic co-ordination of succinoglycan with chromium trivalent cations was confirmed based on the differences in the characteristic absorption peaks of succinoglycan and succinoglycan-based metallohydrogel (SCx). The explanation for the adjustment was typically set to SC_{26.4}, and the same peak shift trend occurred for the other SCx. As shown in Figure 3, the FTIR spectrum of succinoglycan exhibited an absorption peak at 3284 cm⁻¹, which corresponded to the O–H stretching band, while the C=O stretching carbonyl ester of the acetate group exhibited an absorption peak at 1728 cm⁻¹. The absorption peaks at 1626 and 1382 cm⁻¹ were attributed to the asymmetric C=O stretching vibration of the succinate and pyruvate functional groups and symmetric stretching vibration of the carboxylate –COO– group from acid residues, respectively [48]. Additionally, the absorption peak at

1082 cm^{-1} was attributed to the asymmetrical C–O–C stretching vibration [47–49]. However, when succinoglycan was mixed with Cr^{3+} cations, $\text{SC}_{26.4}$ absorption peaks at 3284, 1626, and 1082 cm^{-1} were shifted to 3317, 1634, and 1050 cm^{-1} , respectively. This was potentially due to the co-ordination of succinoglycan with Cr^{3+} ions. The shifts in the absorption peaks indicated that interactions occurred between the carboxyl groups of succinoglycan and Cr^{3+} cations. When succinoglycan was co-ordinated with Cr^{3+} cations, the –OH stretching band at 3284 cm^{-1} of succinoglycan was red-shifted significantly to 3317 cm^{-1} due to the metal co-ordination induced by Cr^{3+} . Furthermore, the C=O stretching vibration peak at 1626 cm^{-1} (which was related to succinate and pyruvate within the succinoglycan) was shifted to 1634 cm^{-1} . Additionally, the asymmetrical C–O–C stretching peak by the backbone sugar shifted from 1082 to 1050 cm^{-1} . The shifts of the peaks at 1626 and 1082 cm^{-1} were attributed to the co-ordination of the carboxyl group with Cr^{3+} cations. Moreover, the results also indicated that the –OH group of succinoglycan was mainly involved in co-ordination with the Cr^{3+} cation via the larger shift of the –OH stretching band of succinoglycan. In conclusion, the results indicated that Cr^{3+} cations are strongly co-ordinated with the carboxyl and hydroxyl groups of succinoglycan.

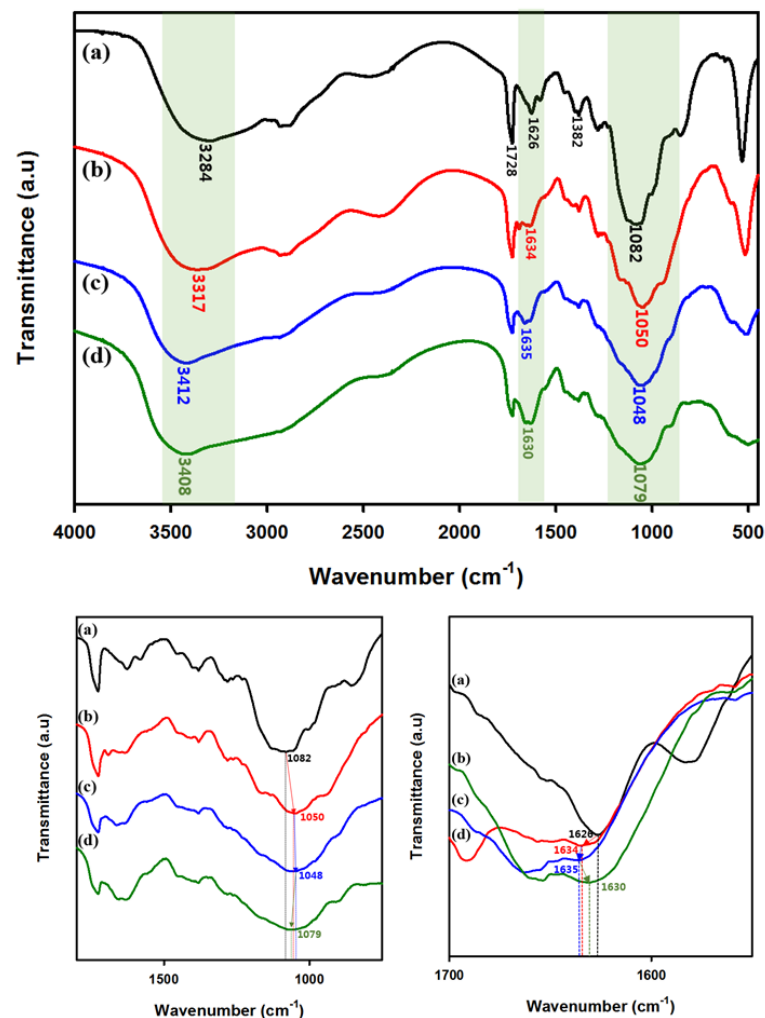


Figure 3. Fourier transform infrared (FTIR) spectra: (a) succinoglycan, (b) $\text{SC}_{13.2}$, (c) $\text{SC}_{26.4}$, and (d) $\text{SC}_{52.8}$.

Figure 4 shows a schematic of the metallohydrogel formation induced by the co-ordination of Cr^{3+} with succinoglycan.

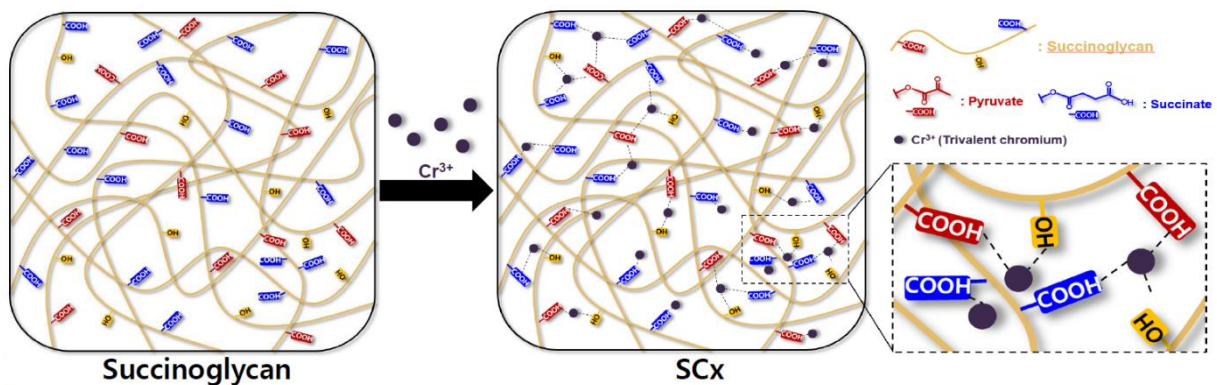


Figure 4. Schematic of a hydrogel crosslinked by complexation of succinoglycan with Cr^{3+} in aqueous solution.

3.3. Analysis of Crystallinity and Diffraction Angle of Metallohydrogels

X-ray diffraction (XRD) measurements were obtained to examine the molecular crystallinity of SCx. As shown in Figure 5, succinoglycan exhibited a large selection at $2\theta = 20.5^\circ$. The diffraction peak of SCx was similar to that of succinoglycan. However, increases in the strength of SCx from $\text{SC}_{6.6}$ to $\text{SC}_{52.8}$ decreased crystallinity. The amorphous region of the succinoglycan polymer matrix was augmented by the addition of Cr^{3+} . This indicates that succinoglycan changes from a crystalline to an amorphous state, thereby indicating that intermolecular hydrogen bonds between metal cations and hydroxyl-/carboxyl groups of succinoglycan occurred for a metallohydrogel [50–52]. The results indicated that the addition of Cr^{3+} changes the intrinsic crystallinity of succinoglycan and generates another regular molecular arrangement.

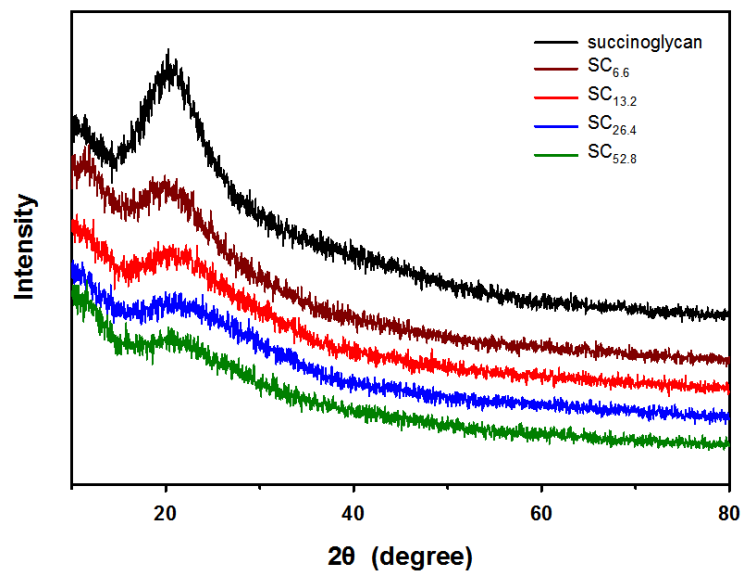


Figure 5. Changes in X-ray diffraction (XRD) patterns of succinoglycan due to hydrogel formation by addition of Cr^{3+} .

3.4. Thermal Analysis of Metallohydrogels

3.4.1. Thermogravimetric Analysis (TGA)

Figure 6 shows TGA and differential thermogravimetry (DTG) diagrams of succinoglycan and SCx. As shown in Figure 6a, the thermal degradation of succinoglycan is divided into two stages. The first mass loss explained the loss of hydrogen bonds and absorbed water molecules attached to the carboxyl group of succinoglycan. The initial moisture content of the samples was attributed to high levels of carboxyl groups of succinoglycan interacting

with water molecules [53]. The result explains the high moisture and water affinity of succinoglycan given its high content of carboxyl groups [54]. In the first stage, the mass loss of succinoglycan and SCx was 8.05% below 95 °C and 10–20% at approximately 110 °C, respectively (Table 2). In the second stage, succinoglycan exhibited a mass loss of 60.64% in the temperature range of 246.14–370.80 °C. In the case of SCx, a second-stage temperature was formed at a lower temperature than that of succinoglycan. With respect to SC_{13.2}, a loss of 53.08% occurred in the temperature range of 213.12–477.24 °C. In particular, SC_{26.4} and SC_{52.8} resulted in mass losses of 49.38% and 38.03% over a wide temperature range of 187.51–484.08 °C and 178.57–480.20 °C, respectively. This was potentially due to the added decomposition of the SCx hydrogel network. Increases in the concentration of Cr³⁺ decreased the final mass loss. Therefore, the mass loss rate of SCx exhibited an inverse relationship with the concentration of Cr³⁺ ions. This indicated that the formation of hydrogels with metals reduced the skeletal degradation of succinoglycan. The results also indicated that the metallohydrogel exhibited better thermal stability than pure succinoglycan.

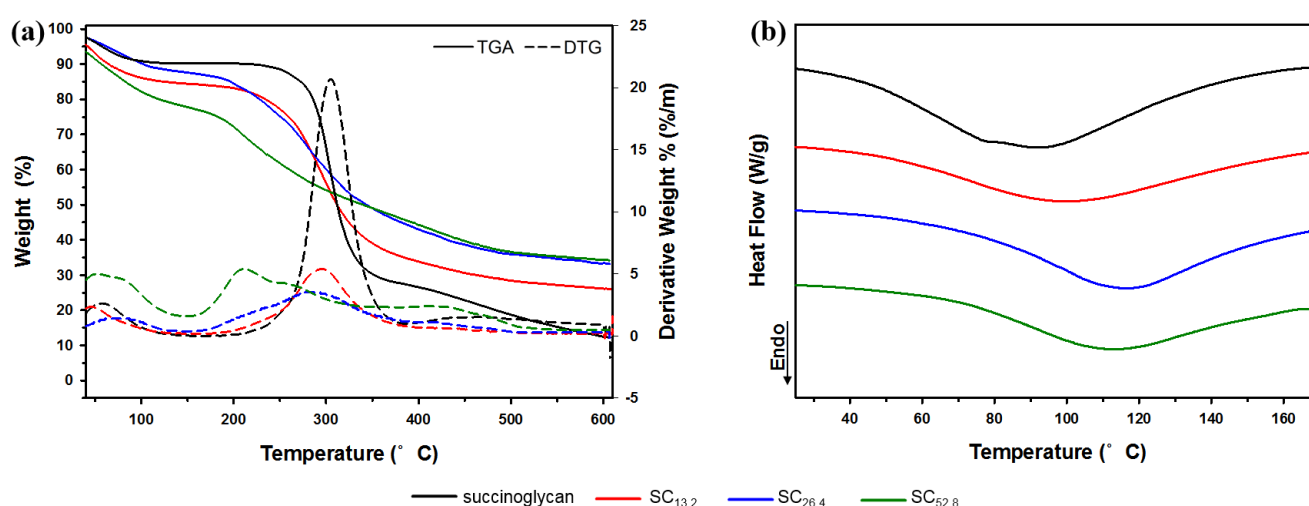


Figure 6. Comparison of the thermal analysis for SCx with respect to different Cr³⁺ concentrations: (a) thermogravimetric analysis (TGA) and (b) differential scanning calorimetry (DSC).

Table 2. Thermal properties of metallohydrogels.

Sample Name	TGA				DSC	
	First Mass Loss Stage	Second Mass Loss Stage		Endothermic Peak		
	Mass Loss (%)	Onset Temperature (°C)	DTG (°C)	Mass Loss (%)	Temperature (°C)	Heat Flow (W/g)
succinoglycan	8.05	246.14	304.98	60.64	92.17	−1.517
SC _{13.2}	12.93	213.12	295.68	53.08	101.40	−1.837
SC _{26.4}	10.47	187.51	285.25	49.38	117.99	−1.829
SC _{52.8}	19.15	178.57	210.95	38.03	114.13	−1.998

3.4.2. DSC Analysis

The DSC curves of succinoglycan and SCx are shown in Figure 6b, and the heat flow values corresponding to the endothermic peak temperature are listed in Table 2. The endothermic peak of DSC is typically due to the breakdown of hydrogen bonds and loss of hydroxyl groups when the sample is heated [55]. In the process of heating, the loss of water attached to the hydroxyl or carboxyl groups of succinoglycan leads to the breakdown of hydrogen bonds inside the hydrogels, which induces the phase transition of SCx. The melting temperature (T_m) generally refers to the transition of the material from a crystalline state to an amorphous state [56], and thus, the transition temperature corresponds to the melting

temperature T_m . As shown in Figure 6b, the melting temperature (T_m) of succinoglycan is observed as 92.17 °C. However, SCx exhibited a change to the maximum T_m corresponding to 117.99 °C based on the concentration of Cr^{3+} . Furthermore, the endothermic enthalpy change (ΔH) increased in SCx when compared to that in succinoglycan. The viscosity of succinoglycan decreased sharply at temperatures exceeding 60 °C (Figure S1). The phenomenon was attributed to the order–disorder conformational transition wherein the chaotic form predominates and the viscosity decreases above 60 °C [57]. The decrease in the molecular weight induced by the irreversible change in viscosity and chain breakage or aggregate breakage can also lead to a difference. The negatively charged carboxyl groups of succinoglycan were co-ordinated with Cr^{3+} , and thus a higher change in enthalpy was required in SCx due to the hydrogel network induced by the addition of Cr^{3+} [53].

3.5. Microstructural Morphology of Metallohydrogels

FESEM images of the fractured surfaces of the hydrogels are shown in Figure 7. The pore size tended to decrease with increases in the concentration of Cr^{3+} , thereby indicating that increases in the amount of Cr^{3+} led to a denser network inside SCx. The result indicated that the concentration of Cr^{3+} plays an important role in co-ordination with succinoglycan. The average pore size of each sample was defined using Image J software (version 1.49v NIH, USA). The pore sizes of SC_{6.6}, SC_{13.2}, SC_{26.4}, and SC_{52.8} corresponded to $215.5 \pm 29 \mu m$, $138.5 \pm 20.5 \mu m$, $125 \pm 32.5 \mu m$, and $203.5 \pm 16.3 \mu m$, respectively. The pore diameter gradually decreased with increases in the concentration of Cr^{3+} and the smallest pore size was observed in SC_{26.4}. Conversely, the pore size of SC_{52.8} exceeded that of SC_{26.4} despite the highest Cr^{3+} concentration. This was potentially due to the electrostatic repulsion inside the network due to an excessive number of Cr^{3+} cations. Thus, the pore size of the obtained SCx can be adjusted by changing the ratio of succinoglycan to (Cr^{3+}).

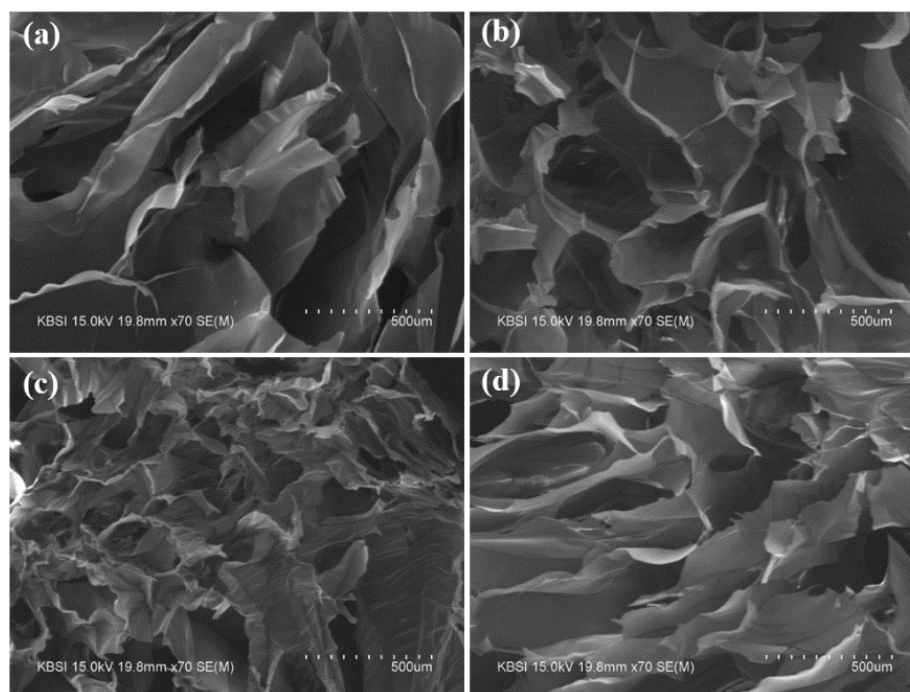


Figure 7. Field emission scanning electron microscopy (FESEM) micrographs of the fractured cross sections of (a) SC_{6.6}, (b) SC_{13.2}, (c) SC_{26.4}, and (d) SC_{52.8}.

3.6. Mechanical Properties of Metallohydrogels

3.6.1. Oscillation Angular Frequency Sweep Test

The viscoelasticity of the hydrogels was evaluated via oscillation angular frequency sweep tests (Figure 8a). The experiment was swept from 0.1 to 100 rad/s at a fixed strain

of 0.5%. The storage modulus (G') corresponds to the value of the resistance to elastic deformation and represents the degree of structuring of the sample. Loss modulus (G'') is a measure of resistance to liquid flow, and it represents the viscosity properties of the test sample [58]. As shown in Figure 8a, all metallohydrogels exhibit storage modulus G' values that exceed those of the loss modulus G'' at a given frequency. This implies that the hydrogel was in the state of an elastic solid gel state and not in a fluid sol state [59]. Increases in the number of crosslinks increase the storage modulus (G') of the hydrogel, thereby indicating that the mechanical properties of the hydrogel depend on the number of crosslinks inside the hydrogel. Increases in the concentration of Cr^{3+} led to a gradual proportional increase in the value of G' . Conversely, it reached the maximum value in $\text{SC}_{26.4}$ and subsequently decreased in $\text{SC}_{52.8}$. Hence, the appropriate amount of Cr^{3+} exhibited a denser and harder hydrogel network due to metal co-ordination with several succinoglycans. Additionally, the results confirmed that the mechanical properties of the resulting metallohydrogel can be controlled by adjusting the concentration of the crosslinking density of SCx.

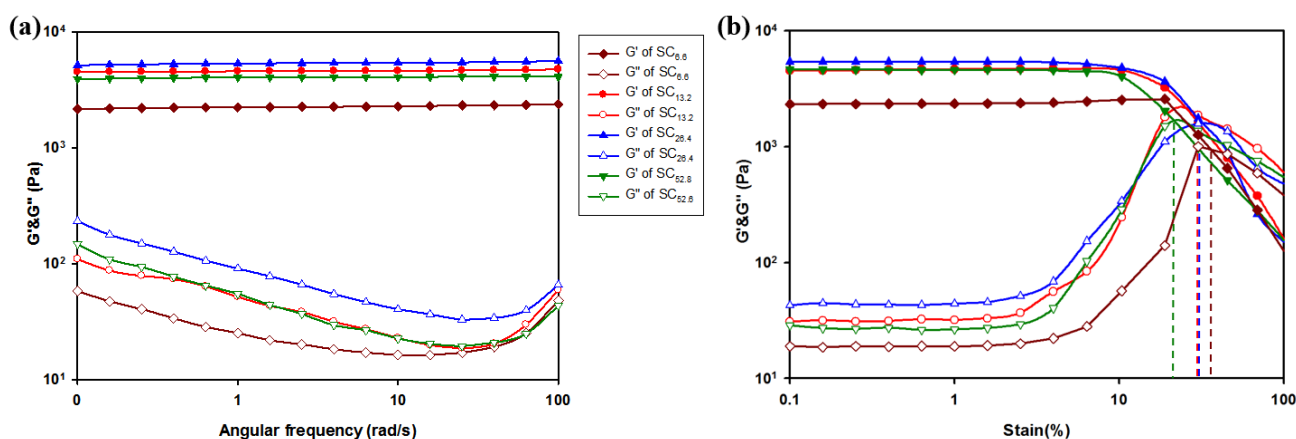


Figure 8. Rheological measurement for SCx: (a) oscillation angular frequency sweep test and (b) stress oscillation strain amplitude sweep test. Storage modulus (G' , filled symbols) and loss modulus (G'' , empty symbols) of hydrogel was measured as a function of angular frequency (0.1–100 rad/s) and strain sweep (0.1–100%).

3.6.2. Stress Oscillation Strain Amplitude Sweep Test

Stress oscillation strain amplitude sweep tests were conducted after fixing the frequency to 1.0 Hz to determine the limit point of the linear viscoelastic region. As shown in Figure 8b, the storage modulus (G') of SCx stays constant in the strain range of 0.1–10%. Thus, this indicates that SCx can withstand high values of shear strain. Furthermore, this implies that SCx retained its gelling properties even at strains as high as 10%. When the strain exceeded 10%, the G' value significantly decreased and the G'' value rapidly increased to generate a crossover point with values corresponding to 36% ($\text{SC}_{6.6}$), 31% ($\text{SC}_{13.2}$), 25% ($\text{SC}_{26.4}$), and 22% ($\text{SC}_{52.8}$). The network of each SCx was completely broken and converted into a sol state at that strain. Hence, the structure of the hydrogel network was completely damaged and exhibited fluid-like properties [60]. The difference in the critical strain values of the four hydrogels was potentially due to the flexibility of the gel network. In particular, $\text{SC}_{52.8}$, with intersections at the lowest strain, indicate hard gels, and $\text{SC}_{6.6}$, with intersections at higher strains, indicate soft gels. Thus, the flexibility of the formed SCx can be controlled by changing the concentration of Cr^{3+} .

3.6.3. Mechanical Properties of SCx in Terms of Compression Strength

Compressive tests were conducted to obtain compressive strain curves for investigating the effect of different Cr^{3+} concentrations on the mechanical properties of SCx (Figure 9). The samples were compared at a strain of 40%. The order of compressive strength for the SCx hydrogel corresponded to $\text{SC}_{26.4}$: 0.1945 MPa > $\text{SC}_{13.2}$: 0.749 MPa > $\text{SC}_{52.8}$: 0.0258 MPa > $\text{SC}_{6.6}$: 0.0190. For SCx, increases in the concentration of Cr^{3+} at 40% strain resulted in

a proportional improvement in compressive strength by approximately 10 times that in the range of 0.0190 MPa ($SC_{6.6}$) to 0.1945 ($SC_{26.4}$). Conversely, $SC_{52.8}$ exhibited a significant decrease in the mechanical strength corresponding to 0.0258 MPa, thereby indicating that electrostatic repulsions can occur inside the network due to excessive concentrations of Cr^{3+} . This indicated that the strongest hydrogel formation occurred at an optimal concentration (26.4 mM) of Cr^{3+} as opposed to the highest concentration. In conclusion, the crosslinking effect of Cr^{3+} was the highest in $SC_{26.4}$, and the results confirmed that the mechanical strength can be effectively improved or controlled by controlling the concentration of Cr^{3+} when preparing a hydrogel with metal.

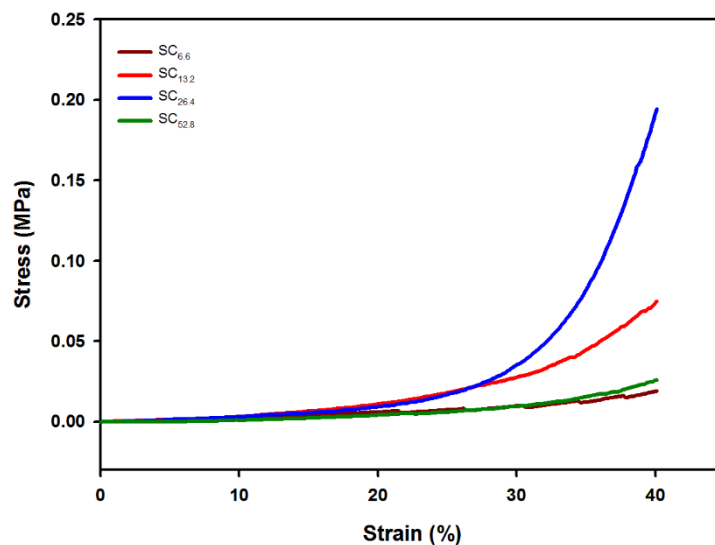


Figure 9. Compressive strain curves of SCx with different Cr^{3+} concentrations.

3.7. Effect of pH of Metallohydrogel on Gelation

The effect of the manufacturing pH on the rheological properties of SCx was examined. As shown in Figure 10a, the range of gel formation was determined by the pH. The experiment was compared by considering six points in the range of pH 1 to 11. The results indicated that G' exceeded G'' in the weak acidic pH range of 3 to 5, thereby indicating that gelation occurred in the pH range of 3–5. However, the sample lost its elastic properties outside the aforementioned range of pH. This is demonstrated by the appearance of the intersection of G' and G'' by changing the rheological behavior (Figure S2). The loss tangent ($\tan\delta$ (G''/G')) is a dimensionless parameter that measures the ratio of energy lost to energy stored in a cyclic deformation [53]. As shown in Figure 10b, strongest hydrogels are formed with the smallest $\tan\delta$ values at pH 5, and this confirms that pH is an important factor that affects the metal co-ordination of succinoglycan and Cr^{3+} . This is related to the nature of interactions based on the structure of the chromium species formed in water and formation of carboxyl groups. In extremely acidic conditions (such as a pH less than 3), Cr^{3+} predominantly exists in the monomeric form, and $(Cr(H_2O)_6)^{3+}$ is co-ordinated with six water molecules [61,62]. Given that the Cr^{3+} monomer is small, it cannot be effectively co-ordinated with the carboxyl group ($pK_a \sim 3.8$) of succinoglycan, where protonation of the carboxylic group can also impede their interactions with Cr^{3+} [63]. However, a higher pH range from 3 to 5 can lead to olate forms of Cr^{3+} (dimeric, trimeric, and tetrameric oligomers), which can lead to successful co-ordination with succinoglycan [43]. In neutral or alkaline conditions with higher pH at which gel formation occurs, chromium ions changed to green in aqueous solution and were converted to water-insoluble hydroxide $Cr(OH)_3$ [64]. In summary, only in the pH range of 3–5 (in which the gel was formed) did Cr^{3+} in the form of olates form an effective co-ordination with the deprotonated carboxyl group of succinoglycan.

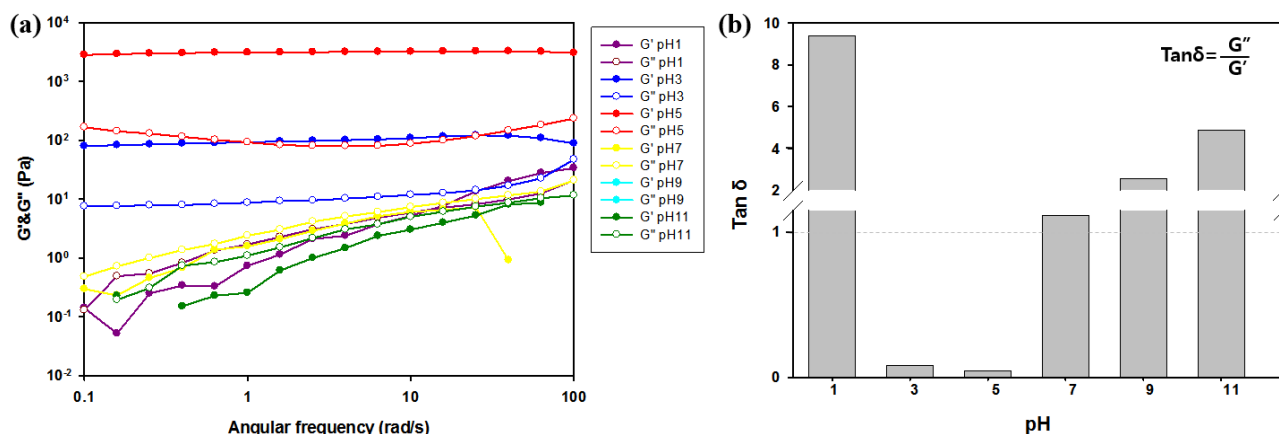


Figure 10. pH-Dependent gelation effect and mechanical properties of SC_{26.4}. (a) Storage modulus (G' , filled symbols) and loss modulus (G'' , empty symbols) of hydrogels. (b) Loss tangent ($\tan \delta$) of hydrogels.

At pH 1, effective crosslinking with succinoglycan did not occur although gel formation was observed as soon as the pH of the solution was changed to 5, and the same phenomenon occurred when the pH of the solution prepared at pH 9 was changed to 5 (Figure S3). The phenomenon can be attributed to the aforementioned pH-dependent behavior of Cr^{3+} .

In both cases, the solution state was changed to a gel state via changes in pH, and rheological properties and mechanical strength were significantly increased (Figure 11a,b). However, the mechanical strength was not completely recovered when compared to that of the hydrogel initially prepared at pH 5 (Figure S4). This was potentially because Cr^{3+} (which corresponded to a monomeric form at a low pH and an insoluble form at a high pH) did not change sufficiently in a short period of time even with a pH change. However, the sample in which pH changed from 5 to a strong acid (pH 1) or strong base (pH 9) remained a gel (Figure 11c,d). A slight increase was observed in the final pH 1 gel because carboxyl groups that were not involved in the crosslinking with Cr^{3+} became uncharged, thereby decreasing counter ion pressure and the swelling degree of the gel [43]. The results indicate that Cr^{3+} and succinoglycan are strongly crosslinked, and thus, the already crosslinked metallohydrogel is less affected by pH.

3.8. Swelling Behavior of Metallohydrogel

The swelling ability of a hydrogel is an important parameter in evaluating its properties. The swelling ratio of SC_x was examined in distilled water at 25 °C and plotted with respect to time. As shown in Figure S5, the swelling ratio of SC_x increases rapidly and then reaches an equilibrium after 5 min. Further, the swelling ratio decreased with increases in the concentrations of Cr^{3+} . The mechanism underlying the phenomenon was closely related to crosslink density. The mechanism underlying the phenomenon was closely related to high crosslinking density due to the excessive concentration of Cr^{3+} , which inhibits the hydrophilicity of succinoglycan by co-ordinating with the O-H bonds of succinoglycan, thereby suppressing the swelling [34]. Additionally, a UV-Vis spectrophotometer was used to confirm whether chromium ions were released after immersion in distilled water (Figure S6). Spectra were observed from 200 to 700 nm at 2 h intervals over 48 h. Peaks did not appear in the solution immersed in SC_x, as shown in Figure S6, where the intrinsic peaks of the Cr^{3+} (5 mM) solution appeared at 570 nm and 415 nm. This confirmed that Cr^{3+} did not release Cr^{3+} when combined with succinoglycan. The results confirmed that Cr^{3+} in the hydrogel was not released even if swelling proceeded.

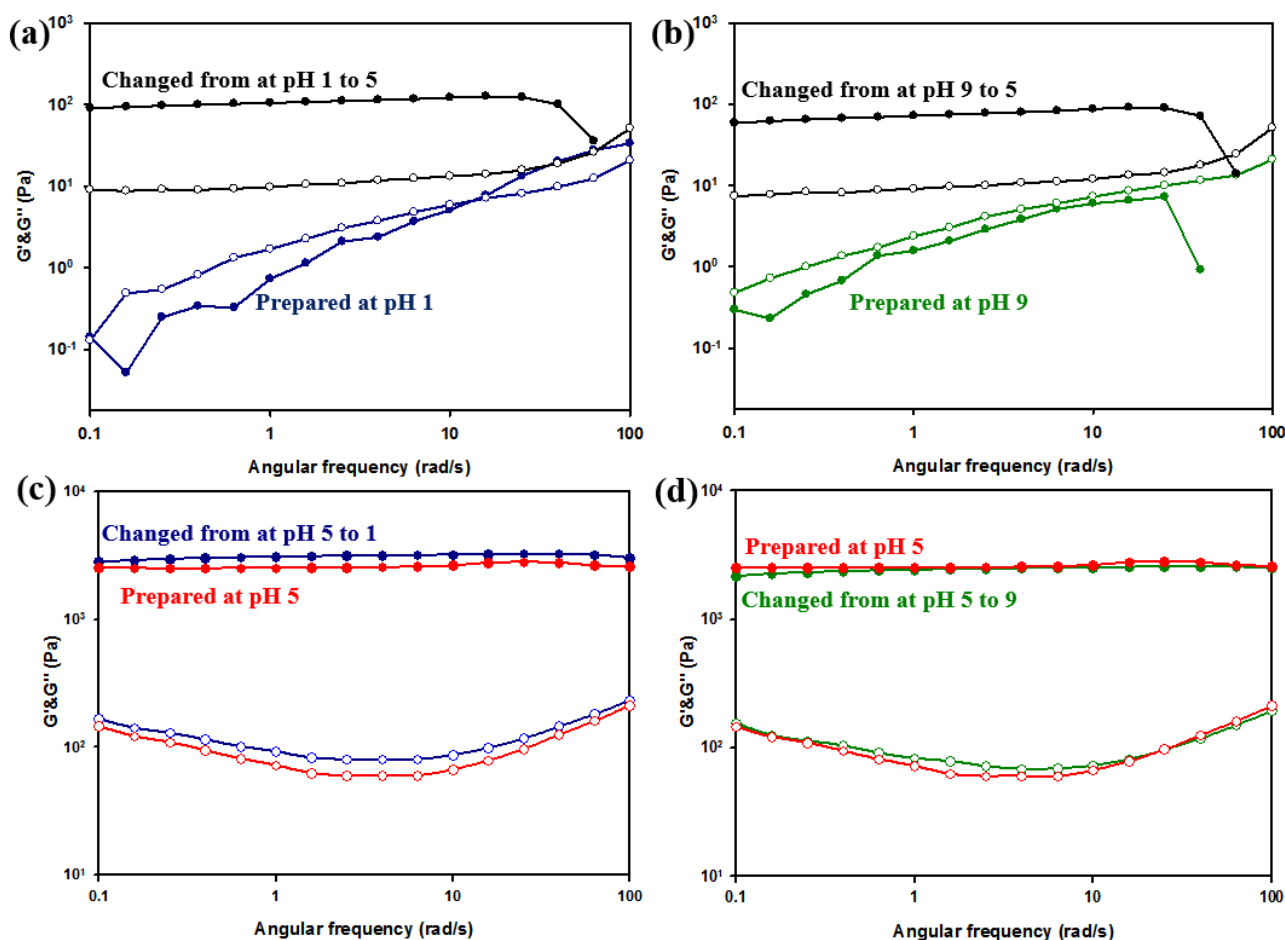


Figure 11. Gelation effect and mechanical properties of SC_{26.4} based on pH changes: (a) from pH 1 to 5, (b) from pH 9 to 5, (c) from pH 5 to 1, and (d) from pH 5 to 9. Storage modulus (G' , filled symbols) and loss modulus (G'' , empty symbols) of hydrogels were measured as a function of angular frequency (0.1–100 rad/s).

4. Conclusions

In this study, succinoglycan-based metallohydrogels (SC_x) were successfully obtained via the metal co-ordination of Cr³⁺ with succinoglycan. Among other metal ions, Cr³⁺ effectively formed a co-ordinated metallohydrogel with succinoglycan at lower concentrations. The characteristics of SC_x were investigated via FTIR, XRD, TGA, DSC, FESEM, and rheological measurements. In particular, FTIR spectroscopy confirmed that the carboxyl and hydroxyl groups of succinoglycan played an important role in metal co-ordination. The change in the thermal stability of succinoglycan was observed via performing TGA and DSC. The results were confirmed by decreases in final weight loss with increases in the concentration of Cr³⁺ (6.6–52.8 mM). Rheological measurements and FESEM indicated that pore size and mechanical properties can be controlled by adjusting the concentration of Cr³⁺. Additionally, succinoglycan metallohydrogellation occurred in a pH-dependent manner. Gelation can also be adjusted based on the initial pH of the hydrogel formulation. A gel was obtained when the pH at preparation ranged from 3 to 5. Furthermore, when the pH of the solution was in the range of 1–9, the pH changed to 5 and gelation occurred. However, crosslinking of the gel was not affected when the gel was stably formed at pH 5 even if the pH was subsequently changed to strongly acidic or basic. This indicated that when crosslinking of the hydrogel with metal is formed, it is stable even under extreme pH conditions. This was attributed to the pH-dependent behavior of Cr³⁺ in aqueous solutions and to the carboxyl groups of succinoglycan that affect metal co-ordination.

In conclusion, the pH-dependent metallohydrogel could increase the thermal stability of succinoglycan, control pore size as well as mechanical strength by adjusting the

concentration of Cr^{3+} . It could be used as a new soft matrix for bioseparation by tuning the Cr^{3+} concentration to control pore size and mechanical strength. In addition, the proposed pH-dependent metallohydrogel offers a promising method for the controllable gelation of succinoglycan with a metal ion and might be applied to monitor Cr^{3+} in drinking water or living cells.

Supplementary Materials: The following are available online at <https://www.mdpi.com/2073-4360/13/2/202/s1>: Table S1. The molecular weight and GPC measurement of succinoglycan; Figure S1: Viscosity change during the first heating cycle of succinoglycan; Figure S2: The pH-dependent gelling effect of an aqueous succinoglycan solution based on Cr^{3+} concentration change; Figure S3: Reversible gel phase transition of SCx hydrogel triggered by a pH change; Figure S4: Comparison of mechanical properties of SC_{26.4} after the changes in pH of solutions initially prepared in strong acids (pH 1) and strong bases (pH 9); Figure S5: Swelling ratio curves for SCx in distilled water at 25 °C; Figure S6: UV-Vis spectra of Cr^{3+} solution (5 mM) and SCx immersed in D.W.

Author Contributions: D.K. performed the experiments and wrote the paper; S.K. performed the methodology; S.J. conceived and designed the experiments. All authors have read and agreed to the published version of the manuscript.

Funding: This paper was supported by Konkuk University in 2019.

Conflicts of Interest: The authors declare no conflict of interest.

References

1. Borisova, A.; De Bruyn, M.; Budarin, V.L.; Shuttleworth, P.S.; Dodson, J.R.; Segatto, M.L.; Clark, J.H. A sustainable freeze-drying route to porous polysaccharides with tailored hierarchical meso- and macroporosity. *Macromol. Rapid Commun.* **2015**, *36*, 774–779. [[CrossRef](#)] [[PubMed](#)]
2. Singh, R.S.; Kaur, N.; Rana, V.; Kennedy, J.F. Pullulan: A novel molecule for biomedical applications. *Carbohydr. Polym.* **2017**, *171*, 102–121. [[CrossRef](#)] [[PubMed](#)]
3. Singh, R.S.; Kaur, N.; Rana, V.; Kennedy, J.F. Recent insights on applications of pullulan in tissue engineering. *Carbohydr. Polym.* **2016**, *153*, 455–462. [[CrossRef](#)] [[PubMed](#)]
4. Dragan, E.S.; Humelnicu, D.; Dinu, M.V.; Olariu, R.I. Kinetics, equilibrium modeling, and thermodynamics on removal of Cr (VI) ions from aqueous solution using novel composites with strong base anion exchanger microspheres embedded into chitosan/poly (vinyl amine) cryogels. *Chem. Eng. J.* **2017**, *330*, 675–691. [[CrossRef](#)]
5. White, R.J.; Shuttleworth, P.S.; Budarin, V.L.; De Bruyn, M.; Fischer, A.; Clark, J.H. An Interesting Class of Porous Polymer—Revisiting the Structure of Mesoporous α -D-Polysaccharide Gels. *ChemSusChem* **2016**, *9*, 280–288. [[CrossRef](#)]
6. Alvarez-Lorenzo, C.; Blanco-Fernandez, B.; Puga, A.M.; Concheiro, A. Crosslinked ionic polysaccharides for stimuli-sensitive drug delivery. *Adv. Drug Deliv. Rev.* **2013**, *65*, 1148–1171. [[CrossRef](#)]
7. García-González, C.A.; Alnaief, M.; Smirnova, I. Polysaccharide-based aerogels—Promising biodegradable carriers for drug delivery systems. *Carbohydr. Polym.* **2011**, *86*, 1425–1438. [[CrossRef](#)]
8. Hu, X.; Pang, X.; Wang, P.G.; Chen, M. Isolation and characterization of an antioxidant exopolysaccharide produced by *Bacillus* sp. S-1 from Sichuan Pickles. *Carbohydr. Polym.* **2019**, *204*, 9–16. [[CrossRef](#)]
9. Andhare, P.; Goswami, D.; Delattre, C.; Pierre, G.; Michaud, P.; Pathak, H. Edifying the strategy for the finest extraction of succinoglycan from *Rhizobium radiobacter* strain CAS. *Appl. Biol. Chem.* **2017**, *60*, 339–348. [[CrossRef](#)]
10. Wahid, F.; Zhou, Y.N.; Wang, H.S.; Wan, T.; Zhong, C.; Chu, L.Q. Injectable self-healing carboxymethyl chitosan-zinc supramolecular hydrogels and their antibacterial activity. *Int. J. Biol. Macromol.* **2018**, *114*, 1233–1239. [[CrossRef](#)]
11. Agulhon, P.; Robitzer, M.; Habas, J.P.; Quignard, F. Influence of both cation and alginate nature on the rheological behavior of transition metal alginate gels. *Carbohydr. Polym.* **2014**, *112*, 525–531. [[CrossRef](#)] [[PubMed](#)]
12. Mikshina, P.V.; Makshakova, O.N.; Petrova, A.A.; Gaifullina, I.Z.; Idiyatullin, B.Z.; Gorshkova, T.A.; Zuev, Y.F. Gelation of rhamnogalacturonan I is based on galactan side chain interaction and does not involve chemical modifications. *Carbohydr. Polym.* **2017**, *171*, 143–151. [[CrossRef](#)] [[PubMed](#)]
13. Bercea, M.; Biliuta, G.; Avadanei, M.; Baron, R.I.; Butnaru, M.; Coseri, S. Self-healing hydrogels of oxidized pullulan and poly (vinyl alcohol). *Carbohydr. Polym.* **2019**, *206*, 210–219. [[CrossRef](#)] [[PubMed](#)]
14. Cai, Z.; Wu, J.; Wu, M.; Li, R.; Wang, P.; Zhang, H. Rheological characterization of novel carboxymethylated curdlan-silica hybrid hydrogels with tunable mechanical properties. *Carbohydr. Polym.* **2020**, *230*, 115578. [[CrossRef](#)]
15. Nair, R.; Choudhury, A.R. Synthesis and rheological characterization of a novel shear thinning levan gellan hydrogel. *Int. J. Biol. Macromol.* **2020**, *159*, 922–930. [[CrossRef](#)]
16. Stredansky, M.; Conti, E.; Bertocchi, C.; Matulova, M.; Zanetti, F. Succinoglycan production by *Agrobacterium tumefaciens*. *J. Ferment. Bioeng.* **1998**, *85*, 398–403. [[CrossRef](#)]

17. Simsek, S.; Wood, K.; Reuhs, B.L. Structural analysis of succinoglycan oligosaccharides from *Sinorhizobium meliloti* strains with different host compatibility phenotypes. *J. Bacteriol.* **2013**, *195*, 2032–2038. [CrossRef]
18. Halder, U.; Banerjee, A.; Bandopadhyay, R. Structural and functional properties, biosynthesis, and patenting trends of Bacterial succinoglycan: A review. *Indian J. Microbiol.* **2017**, *57*, 278–284. [CrossRef]
19. Moosavi-Nasab, M.; Taherian, A.R.; Bakhtiyari, M.; Farahnaky, A.; Askari, H. Structural and rheological properties of succinoglycan biogums made from low-quality date syrup or sucrose using agrobacterium radiobacter inoculation. *Food Bioprocess Technol.* **2012**, *5*, 638–647. [CrossRef]
20. Brenner, T.; Hayakawa, F.; Ishihara, S.; Tanaka, Y.; Nakauma, M.; Kohyama, K.; Nishinari, K. Linear and nonlinear rheology of mixed polysaccharide gels. Pt. II. Extrusion, compression, puncture and extension tests and correlation with sensory evaluation. *J. Texture Stud.* **2014**, *45*, 30–46. [CrossRef]
21. Dong, H.; Snyder, J.F.; Williams, K.S.; Andzelm, J.W. Cation-induced hydrogels of cellulose nanofibrils with tunable moduli. *Biomacromolecules* **2013**, *14*, 3338–3345. [CrossRef] [PubMed]
22. Sun, Z.; Lv, F.; Cao, L.; Liu, L.; Zhang, Y.; Lu, Z. Multistimuli-responsive, moldable supramolecular hydrogels cross-linked by ultrafast complexation of metal ions and biopolymers. *Angew. Chem.* **2015**, *127*, 8055–8059. [CrossRef]
23. Giammanco, G.E.; Sosnofsky, C.T.; Ostrowski, A.D. Light-responsive iron (III)–polysaccharide coordination hydrogels for controlled delivery. *ACS Appl. Mater. Interfaces* **2015**, *7*, 3068–3076. [CrossRef] [PubMed]
24. Moritaka, H.; Fukuba, H.; Kumeno, K.; Nakahama, N.; Nishinari, K. Effect of monovalent and divalent cations on the rheological properties of gellan gels. *Food Hydrocoll.* **1991**, *4*, 495–507. [CrossRef]
25. Abed, A.; Assoul, N.; Ba, M.; Derkaoui, S.M.; Portes, P.; Louedec, L.; Meddahi-Pellé, A. Influence of polysaccharide composition on the biocompatibility of pullulan/dextran-based hydrogels. *J. Biomed. Mater. Res. Part A* **2011**, *96*, 535–542. [CrossRef]
26. Guo, J.; Ge, L.; Li, X.; Mu, C.; Li, D. Periodate oxidation of xanthan gum and its crosslinking effects on gelatin-based edible films. *Food Hydrocoll.* **2014**, *39*, 243–250. [CrossRef]
27. Williams, P.D.; Sadar, L.N.; Martin Lo, Y. Texture stability of hydrogel complex containing curdlan gum over multiple freeze–thaw cycles. *J. Food Process. Preserv.* **2009**, *33*, 126–139. [CrossRef]
28. Sikorski, P.; Mo, F.; Skjåk-Bræk, G.; Stokke, B.T. Evidence for egg-box-compatible interactions in calcium–alginate gels from fiber X-ray diffraction. *Biomacromolecules* **2007**, *8*, 2098–2103. [CrossRef]
29. Machida-Sano, I.; Matsuda, Y.; Namiki, H. In vitro adhesion of human dermal fibroblasts on iron cross-linked alginate films. *Biomed. Mater.* **2009**, *4*, 25008. [CrossRef]
30. Agulhon, P.; Markova, V.; Robitzler, M.; Quignard, F.; Mineva, T. Structure of alginate gels: Interaction of diuronate units with divalent cations from density functional calculations. *Biomacromolecules* **2012**, *13*, 1899–1907. [CrossRef]
31. Barrett, D.G.; Fullenkamp, D.E.; He, L.; Holten-Andersen, N.; Lee, K.Y.C.; Messersmith, P.B. pH-based regulation of hydrogel mechanical properties through mussel-inspired chemistry and processing. *Adv. Funct. Mater.* **2013**, *23*, 1111–1119. [CrossRef] [PubMed]
32. Wahid, F.; Wang, H.S.; Zhong, C.; Chu, L.Q. Facile fabrication of moldable antibacterial carboxymethyl chitosan supramolecular hydrogels cross-linked by metal ions complexation. *Carbohydr. Polym.* **2017**, *165*, 455–461. [CrossRef]
33. Tsutsumi, A.; Ya, D.; Hiraoki, T.; Mochiku, H.; Yamaguchi, R.; Takahashi, N. ESR studies of Mn (II) binding to gellan and carrageenan gels. *Food Hydrocoll.* **1993**, *7*, 427–434. [CrossRef]
34. Su, T.; Qi, X.; Zuo, G.; Pan, X.; Zhang, J.; Han, Z.; Dong, W. Polysaccharide metallohydrogel obtained from Salecan and trivalent chromium: Synthesis and characterization. *Carbohydr. Polym.* **2018**, *181*, 285–291. [CrossRef]
35. Nolte, H.; John, S.; Smidsrød, O.; Stokke, B.T. Gelation of xanthan with trivalent metal ions. *Carbohydr. Polym.* **1992**, *18*, 243–251. [CrossRef]
36. Lund, T.; Smidsrød, O.; Stokke, B.T.; Elgsaeter, A. Controlled gelation of xanthan by trivalent chronic ions. *Carbohydr. Polym.* **1988**, *8*, 245–256. [CrossRef]
37. Grevatt, P. Toxicological Review of Trivalent Chromium. 1998. Available online: <http://www.epa.gov/IRIS/toxreviews/0028-tr.pdf> (accessed on 23 December 2020).
38. Wilbur, S.; Abadin, H.; Fay, M.; Yu, D.; Tencza, B.; Ingerman, L.; James, S. *Toxicological Profile for Chromium*; Agency for Toxic Substances and Disease Registry (US): Atlanta, GA, USA, 2012.
39. Epa, U.S. Integrated Risk Information System (IRIS) on Baygon. In *National Center for Environmental Assessment*; Office of Research and Development: Washington, DC, USA, 1999.
40. Erdemir, S.; Kocuyigit, O. Anthracene excimer-based “turn on” fluorescent sensor for Cr³⁺ and Fe³⁺ ions: Its application to living cells. *Talanta* **2016**, *158*, 63–69. [CrossRef]
41. Jiang, T.; Bian, W.; Kan, J.; Sun, Y.; Ding, N.; Li, W.; Zhou, J. Sensitive and rapid detection of Cr³⁺ in live cells by a red turn-on fluorescent probe. *Spectrochim. Acta Part A Mol. Biomol. Spectrosc.* **2020**, *245*, 118903. [CrossRef] [PubMed]
42. Diao, Q.; Ma, P.; Lv, L.; Li, T.; Wang, X.; Song, D. A novel fluorescent probe for Cr³⁺ based on rhodamine–crown ether conjugate and its application to drinking water examination and bioimaging. *Spectrochim. Acta Part A Mol. Biomol. Spectrosc.* **2016**, *156*, 15–21. [CrossRef] [PubMed]
43. Shibaev, A.V.; Muravlev, D.A.; Muravleva, A.K.; Matveev, V.V.; Chalykh, A.E.; Philippova, O.E. pH-Dependent Gelation of a Stiff Anionic Polysaccharide in the Presence of Metal Ions. *Polymers* **2020**, *12*, 868. [CrossRef] [PubMed]

44. Kolnes, J.; Stavland, A.; Thorsen, S. The effect of temperature on the gelation time of xanthan/Cr (III) systems. In Proceedings of the SPE International Symposium on Oilfield Chemistry, Anaheim, CA, USA, 20–22 February 1991.
45. Cordova, M.; Cheng, M.; Trejo, J.; Johnson, S.J.; Willhite, G.P.; Liang, J.T.; Berkland, C. Delayed HPAM Gelation Via Transient Sequestration of Chromium in Polyelectrolyte Complex Nanoparticles. *Macromolecules* **2008**, *41*, 4398–4404. [[CrossRef](#)]
46. Jeong, D.; Kim, C.; Kim, Y.; Jung, S. Dual crosslinked carboxymethyl cellulose/polyacrylamide interpenetrating hydrogels with highly enhanced mechanical strength and superabsorbent properties. *Eur. Polym. J.* **2020**, *127*, 109586. [[CrossRef](#)]
47. Kang, S.; Lee, S.; Kyung, S.; Jung, S. Catalytic methanolysis induced by succinoglycan, a Rhizobial exopolysaccharide. *Bull. Korean Chem. Soc.* **2006**, *27*, 921.
48. Hu, Y.; Jeong, D.; Kim, Y.; Kim, S.; Jung, S. Preparation of Succinoglycan Hydrogel Coordinated With Fe³⁺ Ions for Controlled Drug Delivery. *Polymers* **2020**, *12*, 977. [[CrossRef](#)] [[PubMed](#)]
49. Chouly, C.; Colquhoun, I.J.; Jodelet, A.; York, G.; Walker, G.C. NMR studies of succinoglycan repeating-unit octasaccharides from *Rhizobium meliloti* and *Agrobacterium radiobacter*. *Int. J. Biol. Macromol.* **1995**, *17*, 357–363. [[CrossRef](#)]
50. Qi, X.; Hu, X.; Wei, W.; Yu, H.; Li, J.; Zhang, J.; Dong, W. Investigation of Salecan/poly (vinyl alcohol) hydrogels prepared by freeze/thaw method. *Carbohydr. Polym.* **2015**, *118*, 60–69. [[CrossRef](#)] [[PubMed](#)]
51. Wei, W.; Li, J.; Qi, X.; Zhong, Y.; Zuo, G.; Pan, X.; Dong, W. Synthesis and characterization of a multi-sensitive polysaccharide hydrogel for drug delivery. *Carbohydr. Polym.* **2017**, *177*, 275–283. [[CrossRef](#)]
52. Singha, N.R.; Mahapatra, M.; Karmakar, M.; Dutta, A.; Mondal, H.; Chattopadhyay, P.K. Synthesis of guar gum-g-(acrylic acid-co-acrylamide-co-3-acrylamido propanoic acid) IPN via in situ attachment of acrylamido propanoic acid for analyzing superadsorption mechanism of Pb (II)/Cd (II)/Cu (II)/MB/MV. *Polym. Chem.* **2017**, *8*, 6750–6777. [[CrossRef](#)]
53. Bakhtiyari, M.; Moosavi-Nasab, M.; Askari, H. Optimization of succinoglycan hydrocolloid production by *Agrobacterium radiobacter* grown in sugar beet molasses and investigation of its physicochemical characteristics. *Food Hydrocoll.* **2015**, *45*, 18–29. [[CrossRef](#)]
54. Kavitate, D.; Delattre, C.; Devi, P.B.; Pierre, G.; Michaud, P.; Shetty, P.H.; Andhare, P. Physical and functional characterization of succinoglycan exopolysaccharide produced by *Rhizobium radiobacter* CAS from curd sample. *Int. J. Biol. Macromol.* **2019**, *134*, 1013–1021. [[CrossRef](#)]
55. Liu, T.; Liu, H.; Fan, H.; Chen, B.; Wang, D.; Sun, F. Preparation and Characterization of a Novel Polysaccharide-Iron (III) Complex in *Auricularia auricula* Potentially Used as an Iron Supplement. *BioMed Res. Int.* **2019**, *2019*, 6416941. [[CrossRef](#)] [[PubMed](#)]
56. Niu, Y.; Xia, Q.; Jung, W.; Yu, L. Polysaccharides-protein interaction of psyllium and whey protein with their texture and bile acid binding activity. *Int. J. Biol. Macromol.* **2019**, *126*, 215–220. [[CrossRef](#)] [[PubMed](#)]
57. Gravanis, G.; Milas, M.; Rinaudo, M.; Clarke-Sturman, A.J. Rheological behaviour of a succinoglycan polysaccharide in dilute and semi-dilute solutions. *Int. J. Biol. Macromol.* **1990**, *12*, 201–206. [[CrossRef](#)]
58. Kim, S.; Jeong, D.; Lee, H.; Kim, D.; Jung, S. Succinoglycan dialdehyde-reinforced gelatin hydrogels with toughness and thermal stability. *Int. J. Biol. Macromol.* **2020**, *149*, 281–289. [[CrossRef](#)] [[PubMed](#)]
59. Yang, X.; Liu, G.; Peng, L.; Guo, J.; Tao, L.; Yuan, J.; Zhang, L. Highly efficient self-healable and dual responsive cellulose-based hydrogels for controlled release and 3D cell culture. *Adv. Funct. Mater.* **2017**, *27*, 1703174. [[CrossRef](#)]
60. Kim, S.; Jung, S. Biocompatible and self-recoverable succinoglycan dialdehyde-crosslinked alginate hydrogels for pH-controlled drug delivery. *Carbohydr. Polym.* **2020**, *250*, 116934. [[CrossRef](#)] [[PubMed](#)]
61. Borchardt, J.K.; Yen, T.F. *Oil-Field Chemistry, ACS Symposium Series*; American Chemical Society: Washington, DC, USA, 1989; pp. 137–144. ISBN 13: 9780841216303.
62. Lockhart, T.P.; Albonico, P.; Burrafato, G. Slow-gelling Cr³⁺/polyacrylamide solutions for reservoir profile modification: Dependence of the gelation time on pH. *J. Appl. Polym. Sci.* **1991**, *43*, 1527–1532. [[CrossRef](#)]
63. Hawkins, J.P.; Geddes, B.A.; Oresnik, I.J. Succinoglycan production contributes to acidic pH tolerance in *Sinorhizobium meliloti* Rm1021. *Mol. Plant-Microbe Interact.* **2017**, *30*, 1009–1019. [[CrossRef](#)]
64. Avena, M.J.; Giacomelli, C.E.; De Pauli, C.P. Formation of Cr (III) hydroxides from chrome alum solutions: 1. Precipitation of active chromium hydroxide. *J. Colloid Interface Sci.* **1996**, *180*, 428–435. [[CrossRef](#)]